Journal of Theoretical Biology 558 (2023) 111370

Contents lists available at ScienceDirect

Journal of Theoretical Biology

journal homepage: www.elsevier.com/locate/yjtbi

Effect of cellular regeneration and viral transmission mode on viral spread

Asher Haun, Baylor Fain, Hana M. Dobrovolny *

Department of Physics & Astronomy, Texas Christian University, Fort Worth, TX, United States of America

ARTICLE INFO

Keywords:
Viral infection
Mathematical model
Agent-based model
Cell-to-cell transmission

ABSTRACT

Illness negatively affects all aspects of life and one major cause of illness is viral infections. Some viral infections can last for weeks; others, like influenza (the flu), can resolve quickly. During infections, uninfected cells can replicate in order to replenish the cells that have died due to the virus. Many viral models, especially those for short-lived infections like influenza, tend to ignore cellular regeneration since many think that uncomplicated influenza resolves much faster than cells regenerate. This research accounts for cellular regeneration, using an agent-based framework, and varies the regeneration rate in order to understand how cell regeneration affects viral infection dynamics under assumptions of different modes of transmission. We find that although the general trends in peak viral load, time of viral peak, and chronic viral load as regeneration rate changes are the same for cell-free or cell-to-cell transmission, the changes are more extreme for cell-to-cell transmission due to limited access of infected cells to newly generated cells.

1. Introduction

Viruses have the ability to infect a broad range of hosts, both plant and animal (Simmonds et al., 2019). The resulting infections generate a wide variety of outcomes, with some infections leading to serious illness or even death in the host, and other infections causing no harm at all to the host (Casadevall and Pirofski, 2018). The time scale of viral infections can also vary widely, ranging from acute infections lasting a few days to chronic infections that last until the host dies of other causes (Sagi and Assaf, 2019).

In the last few decades, mathematical models have been developed to try to capture the varied dynamics of viral infections. While mathematical modeling studies have focused primarily on viral infections causing serious human diseases, such as HIV (Perelson et al., 1997), hepatitis B & C (Li and Zu, 2019; Dixit and Perelson, 2006), influenza (Baccam et al., 2006), and SARS-CoV-2 (Hernandez-Vargas and Velasco-Hernandez, 2020), they have also been applied to plant (Phan et al., 2021) and animal infections (Howey et al., 2012). These models range in complexity, with some capturing only the most basic virus–host interactions and others attempting to incorporate host responses such as innate and adaptive immune responses (Zitzmann and Kaderali, 2018; Murillo et al., 2013).

There is one consistent, clear division, however, between models for acute infections and models for chronic infections — chronic infection models include cell regeneration, while acute infection models neglect this biological reality. The argument for neglecting cell regeneration in acute infections is that the infection is over before a significant number of new target cells appear. The duration of an infection is determined by a number of factors, such as how quickly the virus fuses and enters the cell (Haywood and Boyer, 1986; Mendoza et al., 2020), how quickly it replicates within the cell (Lanahan et al., 2021), how easily it moves between cells (Yang et al., 2014), and the strength of the host immune response (Go et al., 2014, 2019). So while it might be reasonable to neglect cell regeneration for a particular infection in one person, the infection might last long enough in another person to warrant inclusion of cell regeneration for accurate modeling.

In particular, the mode of transmission of the virus could alter the importance of cell regeneration. Recent experimental work has shown that in addition to cell-free transmission, where viruses leave one cell and travel in the extracellular medium to another, viruses are capable of tunneling directly from one cell to another (known as cell-to-cell transmission) (Mothes et al., 2010). Cell regeneration might need to be faster in order to play a role in cell-to-cell transmission dominated infections since new target cells that appear far from the active site of infection are not accessible without cell-free transmission. Mathematical models have started examining the consequences of cell-to-cell transmission (Kumberger et al., 2018; Durso-Cain et al., 2021; Allen and Schwartz, 2015), but have not yet examined how cell regeneration affects viral dynamics for infections using this form of viral transmission.

Modeling studies have previously examined how cell regeneration alters viral dynamics under the assumption of cell-free transmission. Inclusion of cell regeneration in mathematical models is required to

* Corresponding author.
E-mail address: h.dobrovolny@tcu.edu (H.M. Dobrovolny).

https://doi.org/10.1016/j.jtbi.2022.111370
Received 21 May 2022; Received in revised form 3 November 2022; Accepted 18 November 2022
Available online 30 November 2022

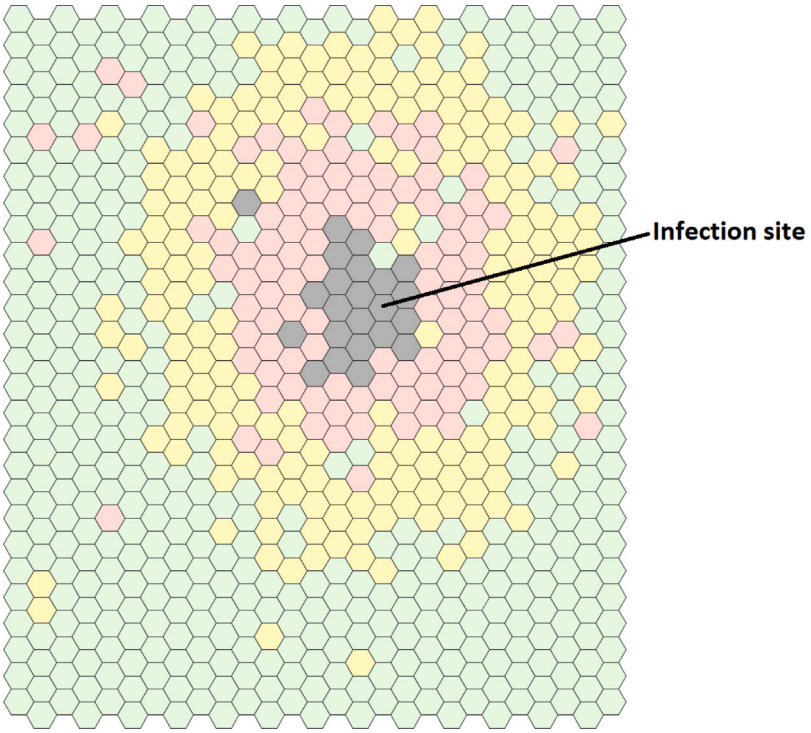

Fig. 1. Visualization of infection spread in the ABM. Each hexagon represents a single cell with color denoting the state of the cell: uninfected (green), eclipse (yellow), infected (red), dead (black).

produce chronic infections, but depending on how it is incorporated into the model does not necessarily lead to chronic infections (Pinky and Dobrovolny, 2017) or can lead to oscillatory viral loads (Eikenberry et al., 2009; Hews et al., 2010). If cell regeneration results in chronic viral infection, the chronic viral load is dependent on the cell regeneration rate (Itakura et al., 2010; Eikenberry et al., 2009; Pinky et al., 2019). Moreover, mathematical modeling has determined that cell regeneration is required, but not sufficient for maintaining chronic viral coinfections (Pinky and Dobrovolny, 2017; Pinky et al., 2019). Finally, cell regeneration can affect treatment options since it is required for intermittent antiviral treatment to work and the rate of cell regeneration alters the optimal cycling parameters (Deecke and Dobrovolny, 2018). These studies make it clear that incorporating cell regeneration into standard viral kinetics models that assume cell-free transmission alters the predicted viral dynamics in clinically important ways.

This research examines the role of cellular regeneration, using a hybrid agent-based model (ABM) and a partial differential equation model (PDM), and varies the regeneration rate in order to understand how cell regeneration affects viral infections. The model used represents how viral infections spread in a two-dimensional layer of cells in order to generate total virus over time graphs for corresponding regeneration rates that can be used to examine how cellular regeneration affects the viral time course in both cell-free and cell-to-cell transmission modes.

2. Model and methods

2.1. Agent-based model

We constructed a hybrid agent based model (ABM) and partial differential equation model (PDM) to simulate the spread of the influenza virus between cells. The base model, which does not account for cellular regeneration, is fully described in Fain and Dobrovolny (2022). The ABM represents each cell individually in a two-dimensional hexagonal grid. The nature of the model allows us to observe the collective behavior of all the cells and graph various properties of the overall simulation such as how many cells have died over time, how many cells have been regenerated, and how many virions are present at any given time.

A visualization of the spatial structure of the ABM model is shown in Fig. 1. As seen in the figure, each cell can be in one of four distinct states ranging from uninfected to dead as follows:

1. Uninfected (green) - The cell contains no virus.
2. Eclipse (yellow) - The cell is infected but is not producing virus.
3. Infected (red) - The cell is releasing virus.
4. Dead (black) - The cell is no longer releasing any virus and is not susceptible to infection.

2.2. Viral infection

We consider two types of viral transmission: cell-free transmission, where virus is released from cells and diffuses to infect other cells; and cell-to-cell transmission, where an infected cell can pass virus directly to an uninfected neighbor. For cell-free transmission, infection of a cell is determined by the amount of virus directly above the cell. The probability per unit time of transitioning from uninfected to eclipse is given by $P_{cf} = 1 - \exp(-\beta V)$, where β is the infection rate and V is the amount of virus directly above the cell. For cell-to-cell transmission, the probability per unit time of an infected cell causing infection of a neighboring uninfected cell is given by P_{c2c} where $P_{c2c} < 1$. If an uninfected cell has more than one infected neighbor, each neighbor has a probability of P_{c2c} of infecting that cell, so the uninfected cell has a probability of infection of $1 - (1 - P_{c2c})^n$, where n is the number of infected neighbors.

The movement of virus over the cells is described by a partial differential equation model,

$$\frac{\partial V(x,y,t)}{\partial t} = D\nabla^2 V(x,y,t) + p - cV(x,y,t),$$

where $V(x,y,t)$ is the amount of virus over the cells, D is the diffusion coefficient, p is the viral production rate, and c is the viral clearance rate. The partial differential equation is solved computationally using the forward Euler method with Neumann boundary conditions.

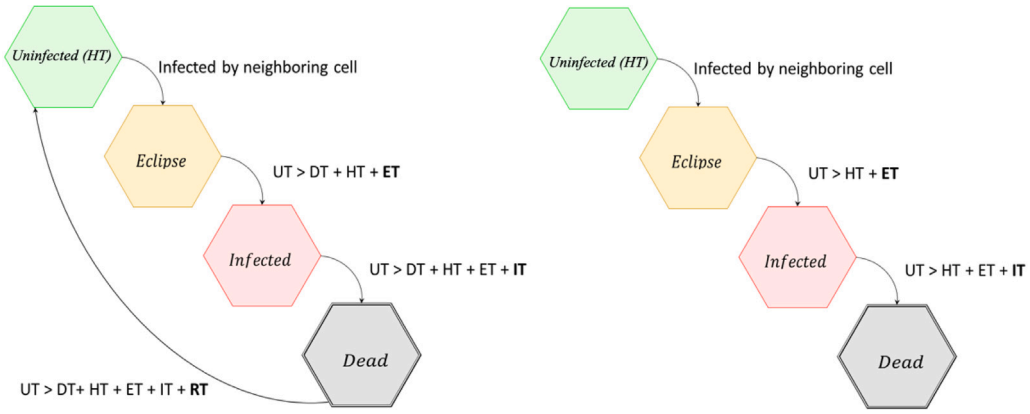

UT	Universal time (simulation time)
HT	Uninfected time
ET	Eclipse time
IT	Infected time
RT	Regeneration time
DT	Dead time (* only added after first regeneration event)

UT	Universal time (simulation time)
HT	Uninfected time
ET	Eclipse time
IT	Infected time

Fig. 2. Mean transition times describing cell phases from uninfected to dead for a model that does not account for cell regeneration (right), and a model that includes the information necessary to account for regeneration (left).

2.3. Cellular regeneration

This manuscript describes an extension of the original model that incorporates cellular regeneration. It is estimated that epithelial cells in the respiratory tract begin proliferating $1-3$ d after injury in hamsters and guinea pigs (Keenan et al., 1983; Erjefalt et al., 1995) to recover from death or injury, although at least one respiratory infection has been shown to delay this response (Linfield et al., 2021). Thus, we examine a range of possible regeneration rates from $0.030-10.000$ /d. In the ABM, after a cell has died, its location in the grid of cells is replaced by a new uninfected cell via mitosis occurring in a neighboring uninfected cell. The probability of a cell being regenerated is determined according to an exponential distribution with a mean regeneration rate r. A cell at a specific location in the grid may only undergo regeneration if it is adjacent to a uninfected cell. This essentially mimics division of the living cell into empty locations in the grid of cells. The mean regeneration rate is the same regardless of how many uninfected neighbors surround a particular cell.

Transitions between states for each cell are shown in Fig. 2. On the right side of Fig. 2, the base simulation model is shown, which does not include cellular regeneration; on the left side, regeneration and the amount of time dead are taken into account — regeneration of a cell in a spot on the grid has the same effect as another cell reproducing into that space on the grid. The times used to transition from eclipse to infectious and from infectious to dead are pulled from Erlang distributions with means τ_E or τ_I and number of stages n_E or n_I respectively. Erlang distributions are used since previous studies have indicated this distribution provides the best fit for these transitions (Beauchemin et al., 2017; Kakizoe et al., 2015). The time used to determine if cellular regeneration should take place is pulled from an exponential distribution.

2.4. Parameters

Parameters are chosen to model influenza infections. The viral infection parameters (β, p, c, τ_I and τ_E) are taken from a fit of this model to in vitro viral titer curves of 2009 pandemic H1N1 influenza (Fain and Dobrovolny, 2022) taken from Pinilla et al. (2012). The diffusion coefficient is calculated using the Stokes–Einstein equation (as in Quirouette et al., 2020). The number of stages in the Erlang distributions for eclipse-infectious and infectious-dead transitions are taken from Pinilla et al. (2012). Parameter values are given in Table 1.

2.5. Simulations

The following information is recorded every hour: number of cells in each phase (uninfected, eclipse, infected, dead) and the total virions present in the dish. Since it is difficult to compare entire time courses, we measure specific aspects of the viral titer time course to easily compare dynamics during cell-to-cell or cell-free transmission. We measure the peak viral load, the time of peak viral load, and the chronic viral load. The peak viral load and chronic load are indicative of the severity of the infection while the time of peak reflects how quickly the infection takes hold. Quantities are plotted as functions of regeneration rate to assess how cell regeneration affects infections transmitted either cell-to-cell or cell-free. A link to code is available on GitHub at *athaun/cell-regen-influenza-model*.

3. Results

We use the ABM/PDM model to run 100 simulations at different regeneration rates assuming either direct cell-to-cell transmission or cell-free transmission. Images of the infection at several time points for each of the transmission modes are shown in Fig. 3. We show both the entire simulated well (left two columns) and a zoomed in region (right two columns). The majority of cells are initially in the uninfected state (green) with a few cells initially in the eclipse phase (cyan). As the infection proceeds, the eclipse cells move to the infected state (red) and eventually die (black). We see that cell-free transmission (right columns) spreads the infection faster than cell-to-cell transmission (left columns) since virus can move away from the originating cell to infect non-adjacent cells — even after 24 h, we can see that cell-free infection has reached all corners of the well and resulted in most cells moving into the eclipse state. In the next sections, we use the total viral load to examine changes in features of the viral load as described in the Methods.

3.1. Peak viral titer

The mean peak viral load as a function of regeneration rate is shown in Fig. 4 for cell-to-cell transmission (black) and cell-free (red) transmission. As the regeneration rate increases, the peak viral load also increases, especially for the cell-to-cell transmission, although there is a

Table 1
Influenza parameters used in the simulation.

Parameter	Description	Value
MOI	Multiplicity of Infection	10^{-2}
β	Infection rate	54 virions^{-1} h^{-1}
p	Virus production rate	3000 virions cells^{-1} h^{-1}
D	Diffusion coefficient	2.2×10^{-8} m^2 h
c	Clearance rate (rate of viral decay)	0.25 h^{-2}
Δx	Cell size	25×10^{-6} m
Δt	Base time step	$2\Delta x$
τ_I	Average time for infectious stage	26.0 h
τ_E	Average time for eclipse stage	16.0 h
n_E	Number of stages in Erlang distribution	30.0
n_I	Number of stages in Erlang distribution	100.0
P_{c2c}	Probability that virus will spread via direct cell-to-cell infection per hour.	0.2 h

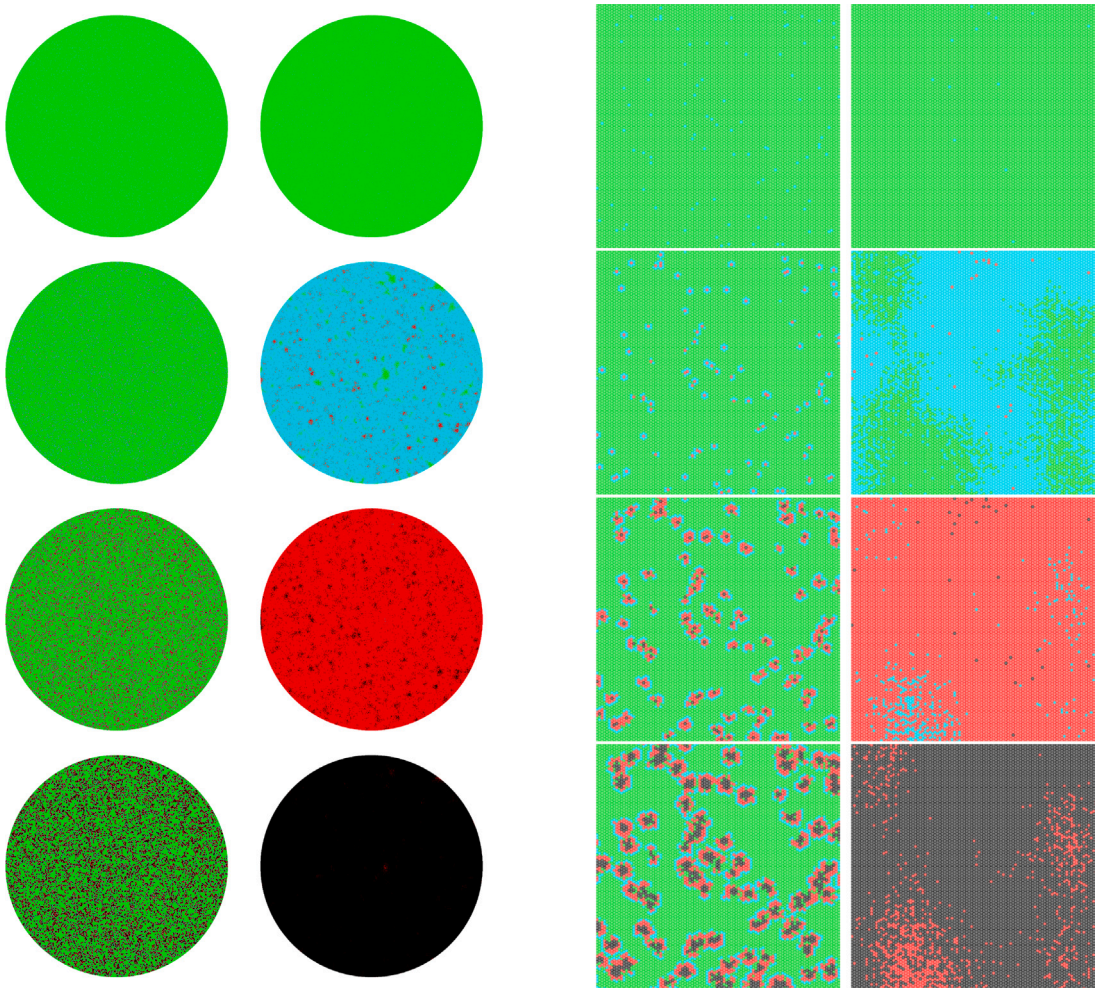

Fig. 3. Simulated influenza infection via cell-to-cell transmission only (left column) or cell-free transmission only (right column). We show the entire simulated well in the left two columns and a zoomed in region in the right two columns. Snapshots are taken at day 0 (top row), day 1 (second row), day 3 (third row), and day 4 (bottom row). Uninfected cells are green; cells in the eclipse phase are cyan; infected cells are red; and dead cells are black. Simulations are run with the parameters given in Table 1.

slight increase in the peak viral load of cell-free transmission at a regeneration rate of $\sim$ 2–3 /d. As the regeneration rate increases, more cells are susceptible to infection, some possibly early enough to contribute to increasing peak viral load when the regeneration rate is fast enough. Note, however, that the changes in peak viral load measured here are all within one log, so might not be experimentally measurable, given the typical error associated with viral load measurements (LaBarre and Lowy, 2001).

We also notice that cell-to-cell transmission always results in a lower peak viral load than cell-free transmission. This is because cell-to-cell transmission overall infects fewer cells than cell-free infection — note that viral production rate is the same for both modes of transmission. In the case of cell-free transmission, if a newly generated cell happens to appear far away from the site of active infection, it can still become infected because of viral diffusion over the entire dish. However, if only cell-to-cell transmission occurs, this newly generated cell will only become infected if there is a bridge of uninfected cells connecting this cell to the site of infection, or if such a bridge forms at some later time. Creating these direct links becomes more difficult as the regeneration rate is lowered since the site of active infection moves further away from the region where cell regeneration is likely to occur, so we see

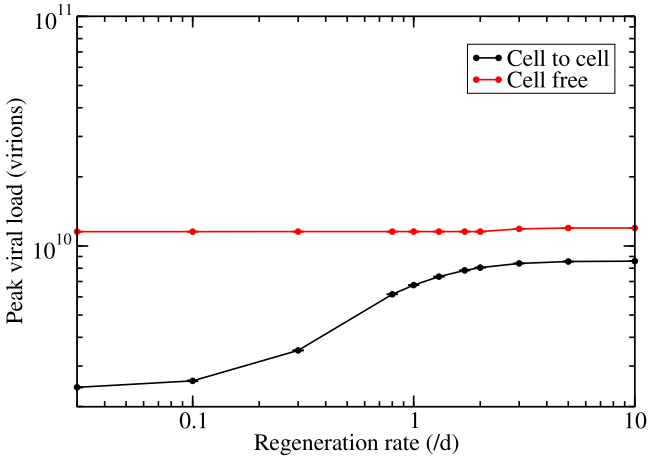

Fig. 4. Peak viral load dependence on cellular regeneration rate for cell-to-cell transmission (black) and cell-free transmission (red).

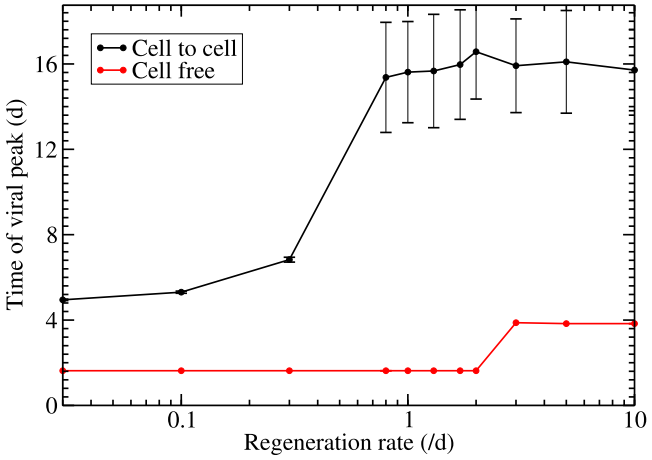

Fig. 5. Time of viral peak dependence on regeneration rate for cell-to-cell transmission (black) and cell-free transmission (red). Error bars are the standard deviation of 100 runs.

a larger divergence in the peak viral load between cell-to-cell and cell-free transmission at lower regeneration.

3.2. Time of viral peak

While the peak viral load can give a measure of the severity of the infection, the time of viral peak indicates how quickly the infection has spread. The time of viral peak is shown as a function of regeneration rate for both cell-to-cell and cell-free transmission in Fig. 5. In both cell-to-cell and cell-free transmission, the time of peak stays relatively steady at low regeneration rates until the regeneration rate is increased to above $\sim 1.7 - 2.0$ /d for cell-free transmission and ~ 0.8 /d for cell-to-cell transmission, where it spikes up and plateaus for both.

We again note some differences between cell-to-cell and cell-free transmission. At all regeneration rates, the time of viral peak occurs later when there is only cell-to-cell transmission. Cell-to-cell transmission generally takes longer to infect a given number of cells since the infection can only be passed to nearest neighbors, so it takes longer to reach the peak viral load. We also see that for cell-free transmission, the time of peak is quite consistent (small standard deviations), however for the cell-to-cell transmission model, the time of peak ranges approximately ± 2 days at higher cell regeneration rates. Stochasticity is partially removed in cell-free transmission since the virus diffuses over the surface of the cells and can skip over regions of dead cells

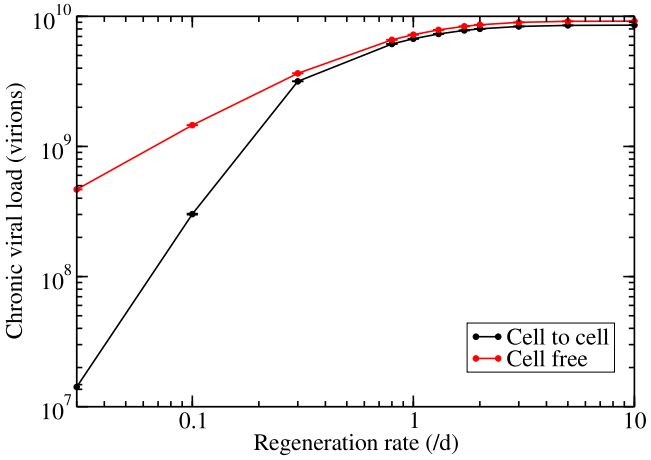

Fig. 6. Chronic viral load dependence on regeneration rate for cell-to-cell transmission (black) and cell-free transmission (red). Error bars are the standard deviation of 100 runs.

to continuously infect cells. During cell-to-cell transmission, a virus' ability to spread consistently might be hindered by the exact spatial distribution of infected cells and dead cells leading to more variation in the time of viral peak.

3.3. Chronic viral load

With cell regeneration providing a consistent supply of new cells, our model predicts chronic infections. The severity of chronic infections can be assessed by measuring the chronic viral load. The chronic viral load is shown in Fig. 6 for different regeneration rates for both cell-to-cell (black line) and cell-free (red line) transmission. As the cellular regeneration rate increases, the amount of virus present in the chronic infection also increases. Since cells are continuously being regenerated, there are more cells to infect compared to a model that does not account for regeneration, allowing the infection to become chronic.

While cell-to-cell transmitted infections and cell-free transmitted infections converge to similar viral loads at high regeneration rates, at low regeneration rates, the chronic viral load is lower for cell-to-cell transmitted infections. This is because new cells might appear at locations that are not near infected cells, meaning that they are not immediately accessible for infection. As regeneration rate increases, this difference in chronic load for different transmission mechanisms disappears. As the regeneration rate passes 1.0 /d the chronic load begins to plateau, this is due to the dish of cells reaching capacity where the chronic load is close to the peak viral load.

3.4. Effect of antivirals

We also used the model to examine the effect of antivirals on the infection. The primary class of antivirals currently in use against influenza is the neuraminidase inhibitors (NAIs). NAIs block release of virus (Abed et al., 2002; Gubareva et al., 2000) and are typically modeled as reducing the production rate (Dobrovolny et al., 2011; Handel et al., 2007; Palmer et al., 2017; Cao and McCaw, 2015; Dobrovolny and Beauchemin, 2017; Beggs and Dobrovolny, 2015). We examined the effect of NAIs by looking at a 50% reduction in the production rate, as well as a 98% reduction in production rate. Results are shown in Fig. 7.

For NAIs, we see some obvious differences once the antiviral is applied. The peak viral load and chronic viral load decrease for both transmission modes since the production rate is lower. There is also a slight lengthening of the time of peak viral load for the cell-free transmission mode. While this shift is expected for the cell-free transmission

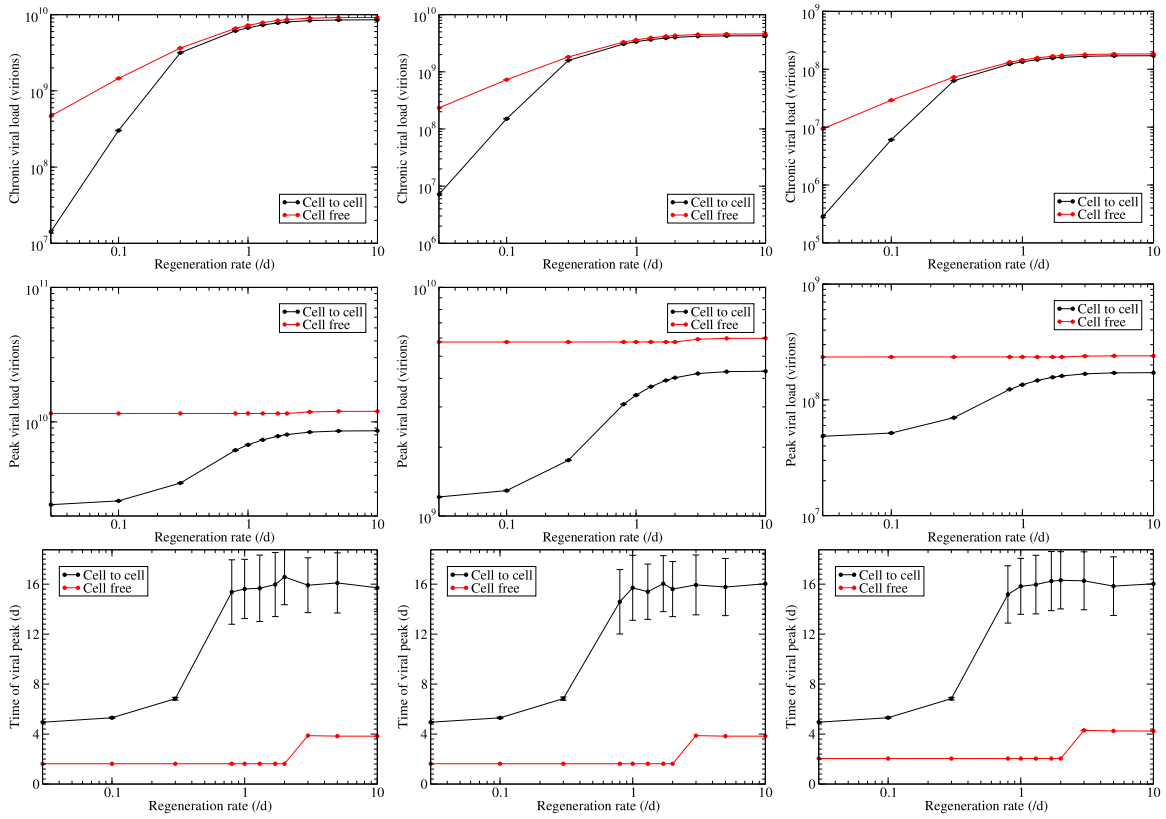

Fig. 7. Effect of NAIs on features of the viral time course in cell-to-cell and cell-free influenza infections. We show the chronic viral load (top row), peak viral load (center row), and time of viral peak (bottom row) as functions of the regeneration rate in the case of no treatment (left column), a 50% reduction in p (center column), and a 98% reduction of p (right column).

mode, we do not expect to see a change in the time of peak for cell-to-cell infection. For cell-to-cell transmission, the production rate does not play a role in spread of the infection, so we do not expect a change in the underlying dynamics of the cell-to-cell infection. From ordinary differential equation models, the expected effect of NAIs is to lower the peak viral load and delay the time of peak until it reaches the threshold for curing the infection (Beggs and Dobrovolny, 2015). The changes to the time of peak are small until near the threshold, which is determined by the basic reproduction number (Dobrovolny et al., 2011). The basic reproduction number for the Pinilla data is estimated at 1700 (Pinilla et al., 2012), so the drug efficacy required to cure the infection is 99.94%, which is quite a bit higher than the 98% drug efficacy assumed here and might be the reason we do not see much of a shift.

4. Discussion

By examining the effect that varying rates of cellular regeneration have on peak viral load, time of peak virus, and chronic viral load, it is evident that cell regeneration is an important aspect of viral models. Infectious models that do not account for regeneration are by their nature short lived—this is due to the fact that in a model that ignores the biological reality of regeneration, potential target cells are unrealistically discarded. While neglecting cell regeneration might work well for modeling acute infections in healthy patients, it is inherently ascribing the cause of infection resolution to the wrong mechanism (Cao and McCaw, 2015). In healthy adults, acute infections such as influenza are thought to be resolved because of the immune response rather than death of all susceptible cells (Beauchemin and Handel, 2011). Even with low regeneration rates, our model predicts long-lasting infections, suggesting that the more accurate model for acute infections includes regeneration with the infection being suppressed by an immune response (Dobrovolny et al., 2013).

For both the peak viral load and time of viral peak, we noted that dynamics of the infection shift at regeneration rates around $1.0 - 2.0$ /d. Interestingly, Deecke and Dobrovolny (2018) also found an abrupt change in dynamics of intermittent treatment at a particular regeneration rate, although the dynamical change in their system occurred at a lower regeneration rate than we observe here. It is unclear how these threshold rates of regeneration are relevant for actual infections since it is estimated that epithelial cells in the respiratory tract regenerate at $0.3 - 1$ /d, based on measurements after injury in hamsters and guinea pigs (Keenan et al., 1983; Erjefalt et al., 1995). This is above the threshold rate measured in Deecke and Dobrovolny (2018) and slightly below the threshold rate found here.

As the rate of cell regeneration increases, the severity of the infection also increases as seen by the higher peak viral load and higher chronic viral load for faster regeneration rates. The dependence of chronic viral load on regeneration rate has been noted in other studies (Itakura et al., 2010; Eikenberry et al., 2009). One study also found that coinfection duration is longer at higher regeneration rates when regeneration is included in a model of viral coinfection (Pinky and Dobrovolny, 2017).

We noted some differences in how changes in cell regeneration rate differ based on the mode of transmission of the virus. The observed differences in peak viral load, time of viral peak, and chronic viral load occur because cell-free transmission provides the virus access to all cells in the dish, whereas cell-to-cell transmission only allows the virus to access nearest neighbors. This model examines the effect of cell regeneration on infections that utilize either cell free and cell-to-cell transmission individually; evidence suggests that both forms of transmission occur at the same time during infections (Durso-Cain et al., 2021; Blahut et al., 2021). Interestingly, both studies suggest that most cells are infected via cell-to-cell transmission, with cell-free transmission's main role being to seed infections in new infection-free

locations. Thus, so long as there is some cell-free transmission, the virus should be able to access and take advantage of newly grown cells. However, this dynamic might change in the presence of antivirals. The two primary classes of antivirals for influenza target processes that are only important for cell-free transmission (viral entry into the cell and viral release from the cell). Thus treatment with antivirals will primarily cut off the long-range transmission of virus, leaving intact the slower cell-to-cell transmission that can potentially prolong the infection.

It is important to acknowledge the limitations of this model. One aspect of viral infections that this model does not take into account is the immune response. The adaptive immune response, which includes cytotoxic T lymphocytes (CTLs) and antibodies (Abs), limits viral load (Nowak and Bangham, 1996), so could suppress an otherwise chronic infection. Thus incorporating an immune response would likely change our chronic infections to acute infections given a sufficiently large immune response. We also chose a fairly low cell-to-cell transmission probability when running our simulations. As this value gets larger, cell-to-cell transmission will spread faster and the differences we observe between the two modes of transmission will lessen. Similarly, changes in the diffusion coefficient will change the speed at which cell-free transmission spreads the infection, with low diffusion coefficients leading to more spatial heterogeneity even for cell-free transmission (Holder et al., 2011).

5. Conclusion

It is apparent that cellular regeneration has an effect on viral infections; however, there is not a significant amount of research being conducted on the effects of regeneration. In particular, we found differences in how cellular regeneration interplays with different types of viral transmission, since viruses transmitting solely via cell-to-cell transmission might not have access to newly regenerated cells. This aspect of viral infections has an impact on viral dynamics even in short lived infections like influenza and more research on the subject should be undertaken.

CRediT authorship contribution statement

Asher Haun: Methodology, Software, Validation, Formal analysis, Data curation, Writing – original draft, Writing – review & editing. **Baylor Fain:** Conceptualization, Methodology, Software, Validation, Formal analysis, Writing – review & editing, Visualization, Supervision. **Hana M. Dobrovolny:** Conceptualization, Methodology, Writing – review & editing, Supervision, Project administration.

Declaration of competing interest

The authors declare that they have no known competing financial interests or personal relationships that could have appeared to influence the work reported in this paper.

Acknowledgment

All authors have read and agreed to the published version of the manuscript.

References

Abed, Y., Bourgault, A.-M., Fenton, R.J., Morley, P.J., Gower, D., Owens, I.J., Tisdale, M., Boivin, G., 2002. Characterization of 2 influenza A(H3N2) clinical isolates with reduced susceptibility to neuraminidase inhibitors due to mutations in the hemagglutinin gene. J. Infect. Dis. 186 (8), 1074–1080.

Allen, L.J., Schwartz, E.J., 2015. Free-virus and cell-to-cell transmission in models of equine infectious anemia virus infection. Math. Biosci. 270, 237–248. http://dx.doi.org/10.1016/j.mbs.2015.04.001.

Baccam, P., Beauchemin, C., Macken, C.A., Hayden, F.G., Perelson, A.S., 2006. Kinetics of influenza A virus infection in humans. J. Virol. 80 (15), 7590–7599. http://dx.doi.org/10.1128/JVI.01623-05.

Beauchemin, C.A., Handel, A., 2011. A review of mathematical models of influenza A infections within a host or cell culture: lessons learned and challenges ahead. BMC Public Health 11 (S1), S7–S22, www.biomedcentral.com/1471-2458-11-S1-S7.

Beauchemin, C.A., Miura, T., Iwami, S., 2017. Duration of SHIV production by infected cells is not exponentially distributed: Implications for estimates of infection parameters and antiviral efficacy. Sci. Rep. 7, 42765. http://dx.doi.org/10.1038/srep42765.

Beggs, N.F., Dobrovolny, H.M., 2015. Determining drug efficacy parameters for mathematical models of influenza. J. Biol. Dyn. 9 (S1), 332–346. http://dx.doi.org/10.1080/17513758.2015.1052764.

Blahut, K., Quirouette, C., Feld, J.J., Iwami, S., Beauchemin, C.A., 2021. Quantifying the relative contribution of free virus and cell-to-cell transmission routes to the propagation of hepatitis c virus infections in vitro using an agent-based model. http://dx.doi.org/10.48550/arXiv.2102.05531, arXiv.

Cao, P., McCaw, J.M., 2015. The mechanisms for within-host influenza virus control affect model-based assessment and prediction of antiviral treatment. Viruses - Basel 9 (8), 197. http://dx.doi.org/10.3390/v9080197.

Casadevall, A., Pirofski, L.-A., 2018. What is a host? attributes of individual susceptibility. Infect. Immun. 86 (2), e00636–17. http://dx.doi.org/10.1128/IAI.00636-17.

Deecke, L.A., Dobrovolny, H.M., 2018. Intermittent treatment of severe influenza. J. Theoret. Biol. 442, 129–138. http://dx.doi.org/10.1016/j.jtbi.2018.01.012.

Dixit, N., Perelson, A., 2006. The metabolism, pharmacokinetics and mechanisms of antiviral activity of ribavirin against hepatitis C virus. Cell. Mol. Life Sci. 63 (7–8), 832–842. http://dx.doi.org/10.1007/s00018-005-5455-y.

Dobrovolny, H.M., Beauchemin, C.A., 2017. Modelling the emergence of influenza drug resistance: The roles of surface proteins, the immune response and antiviral mechanisms. PLoS One 12 (7), e0180582. http://dx.doi.org/10.1371/journal.pone.0180582.

Dobrovolny, H.M., Gieschke, R., Davies, B.E., Jumbe, N.L., Beauchemin, C.A.A., 2011. Neuraminidase inhibitors for treatment of human and avian strain influenza: A comparative study. J. Theoret. Biol. 269 (1), 234–244. http://dx.doi.org/10.1016/j.jtbi.2010.10.017.

Dobrovolny, H.M., Reddy, M.B., Kamal, M.A., Rayner, C.R., Beauchemin, C.A., 2013. Assessing mathematical models of influenza infections using features of the immune response. PLoS One 8 (2), e57088. http://dx.doi.org/10.1371/journal.pone.0057088.

Durso-Cain, K., Kumberger, P., Schalte, Y., Fink, T., Dahari, H., Hasenauer, J., Uprichard, S.L., Graw, F., 2021. HCV spread kinetics reveal varying contributions of transmission modes to infection dynamics. Viruses 13 (7), 1308. http://dx.doi.org/10.3390/v13071308.

Eikenberry, S., Hews, S., Nagy, J.D., Kuang, Y., 2009. The dynamics of a delay model of hepatitis B virus infection with logistic hepatocyte growth. Math. Biosci. Eng. 6 (2), 283–299. http://dx.doi.org/10.3934/mbe.2009.6.283.

Erjefalt, J., Erjefalt, I., Sundler, F., Persson, C., 1995. In-vivo restitution of airway epithelium. Cell Tissue Res. 281 (2), 305–316. http://dx.doi.org/10.1007/BF00583399.

Fain, B., Dobrovolny, H.M., 2022. GPU acceleration and data fitting: Agent-based models of viral infections can now be parameterized in hours. J. Comput. Sci. 61, 101662. http://dx.doi.org/10.1016/j.jocs.2022.101662.

Go, N., Belloc, C., Bidot, C., Touzeau, S., 2019. Why, when and how should exposure be considered at the within-host scale? a modelling contribution to PRRSv infection. Math. Med. Biol. 36 (2), 179–206. http://dx.doi.org/10.1093/imammb/dqy005.

Go, N., Bidot, C., Belloc, C., Touzeau, S., 2014. Integrative model of the immune response to a pulmonary macrophage infection: What determines the infection duration? PLoS One 9 (9), e107818. http://dx.doi.org/10.1371/journal.pone.0107818.

Gubareva, L.V., Kaiser, L., Hayden, F.G., 2000. Influenza virus neuraminidase inhibitors. Lancet 355 (9206), 827–835. http://dx.doi.org/10.1016/S0140-6736(99)11433-8.

Handel, A., L, Jr., I.M., Antia, R., 2007. Neuraminidase inhibitor resistance in influenza: Assessing the danger of its generation and spread. PLoS Comput. Biol. 3 (12), 2456–2464. http://dx.doi.org/10.1371/journal.pcbi.0030240.

Haywood, A., Boyer, B., 1986. Time and temperature dependence of influenza virus membrane fusion at neutral pH. J. Gen. Virol. 67 (12), 2813–2817. http://dx.doi.org/10.1099/0022-1317-67-12-2813.

Hernandez-Vargas, E.A., Velasco-Hernandez, J.X., 2020. In-host modelling of COVID-19 kinetics in humans. Ann. Rev. Contr. 50 (2020), 448–456. http://dx.doi.org/10.1101/2020.03.26.20044487.

Hews, S., Eikenberry, S., Nagy, J.D., Kuang, Y., 2010. Rich dynamics of a hepatitis B viral infection model with logistic hepatocyte growth. J. Math. Biol. 60 (4), 573–590. http://dx.doi.org/10.1007/s00285-009-0278-3.

Holder, B.P., Liao, L.E., Simon, P., Boivin, G., Beauchemin, C.A.A., 2011. Design considerations in building in silico equivalents of common experimental influenza virus assays and the benefits of such an approach. Autoimmunity 44 (4), http://dx.doi.org/10.3109/08916934.2011.523267.

Howey, R., Bankowski, B., Juleff, N., Savill, N.J., Gibson, D., Fazakerley, J., Charleston, B., Woolhouse, M.E., 2012. Modelling the within-host dynamics of the foot-and-mouth disease virus in cattle. Epidemics 4 (2), 93–103. http://dx.doi.org/10.1016/j.epidem.2012.04.001.

Itakura, J., Kurosaki, M., Itakura, Y., Maekawa, S., Asahina, Y., Izumi, N., Enomoto, N., 2010. Reproducibility and usability of chronic virus infection model using agent-based simulation; comparing with a mathematical model. Biosys. 99 (1), 70–78. http://dx.doi.org/10.1016/j.biosystems.2009.09.001.

Kakizoe, Y., Nakaoka, S., Beauchemin, C.A., Morita, S., Mori, H., Igarashi, T., Aihara, K., Miura, T., Iwami, S., 2015. A method to determine the duration of the eclipse phase for in vitro infection with a highly pathogenic SHIV strain. Sci. Rep. 5, 10371. http://dx.doi.org/10.1038/srep10371.

Keenan, K., Wilson, T., McDowell, E., 1983. Regneration of hamster tracheal epithelium after mechanical injury 4. histochemical, immunocytochemical and ultrastructural studies. Vir. Arch. B 43 (3), 213–240. http://dx.doi.org/10.1007/BF02932958.

Kumberger, P., Durso-Cain, K., Uprichard, S.L., Dahari, H., Graw, F., 2018. Accounting for space - quantification of cell-to-cell transmission kinetics using virus dynamics models. Viruses 10 (4), 200. http://dx.doi.org/10.3390/v10040200.

LaBarre, D., Lowy, R., 2001. Improvements in methods for calculating virus titer estimates from $TCID_{50}$ and plaque assays. J. Virol. Meth. 96 (2), 107–126. http://dx.doi.org/10.1016/S0166-0934(01)00316-0.

Lanahan, M.R., Maples, R.W., Pfeiffer, J.K., 2021. Tradeoffs for a viral mutant with enhanced replication speed. Proc. Natl. Acad. Sci. 118 (30), e2105288118. http://dx.doi.org/10.1073/pnas.2105288118.

Li, M., Zu, J., 2019. The review of differential equation models of HBV infection dynamics. J. Virol. Meth. 266, 103–113. http://dx.doi.org/10.1016/j.jviromet.2019.01.014.

Linfield, D.T., Gao, N., Raduka, A., Harford, T.J., Piedimonte, G., Rezaee, F., 2021. RSV attenuates epithelial cell restitution by inhibiting actin cytoskeleton-dependent cell migration. Am. J. Physiol. 321 (1), L189–L203. http://dx.doi.org/10.1152/ajplung.00118.2021.

Mendoza, M.F.L., Acciani, M.D., Levit, C.N., Santa Maria, C., Brindley, M.A., 2020. Monitoring viral entry in real-time using a luciferase recombinant vesicular stomatitis virus producing SARS-CoV-2, EBOV, LASV, CHIKV, and VSV glycoproteins. Viruses 12 (12), 1457. http://dx.doi.org/10.3390/v12121457.

Mothes, W., Sherer, N.M., Jin, J., Zhong, P., 2010. Virus cell-to-cell transmission. J. Virol. 84 (17), 8360–8368. http://dx.doi.org/10.1128/JVI.00443-10.

Murillo, L.N., Murillo, M.S., Perelson, A.S., 2013. Towards multiscale modeling of influenza infection. J. Theoret. Biol. 332, 267–290. http://dx.doi.org/10.1016/j.jtbi.2013.03.024.

Nowak, M.A., Bangham, C.R.M., 1996. Population dynamics of immune responses to persistent viruses. Science 272 (5258), 74–79. http://dx.doi.org/10.1126/science.272.5258.74, arXiv:https://www.science.org/doi/pdf/10.1126/science.272.5258.74.

Palmer, J., Dobrovolny, H.M., Beauchemin, C.A., 2017. The in vivo efficacy of neuraminidase inhibitors cannot be determined from the decay rates of influenza viral titers observed in treated patients. Sci. Rep. 7, 40210. http://dx.doi.org/10.1038/srep40210.

Perelson, A.S., Essunger, P., Cao, Y., Vesanen, M., Hurley, A., Saksela, K., Markowitz, M., Ho, D.D., 1997. Decay characteristics of HIV-1 infected compartments during combination therapy. Nature 387 (6629), 188–191. http://dx.doi.org/10.1038/387188a0.

Phan, T., Pell, B., Kendig, A.E., Borer, E.T., Kuang, Y., 2021. Rich dynamics of a simple delay host-pathogen model of cell-to-cell infection for plant viruses. Disc. Cont. Dyn. Sys. 26 (1), 515–539. http://dx.doi.org/10.3934/dcdsb.2020261.

Pinilla, L.T., Holder, B.P., Abed, Y., Boivin, G., Beauchemin, C.A.A., 2012. The H275Y neuraminidase mutation of the pandemic A/H1N1 influenza virus lengthens the eclipse phase and reduces viral output of infected cells, potentially compromising fitness in ferrets. J. Virol. 86 (19), 10651–10660. http://dx.doi.org/10.1128/JVI.07244-11.

Pinky, L., Dobrovolny, H.M., 2017. The impact of cell regeneration on the dynamics of viral coinfection. Chaos 27 (6), 063109. http://dx.doi.org/10.1063/1.4985276.

Pinky, L., González-Parra, G., Dobrovolny, H.M., 2019. Superinfection and cell regeneration can lead to chronic viral coinfections. J. Theoret. Biol. 466, 24–38. http://dx.doi.org/10.1016/j.jtbi.2019.01.011.

Quirouette, C., Younis, N.P., Reddy, M.B., Beauchemin, C.A.A., 2020. A mathematical model describing the localization and spread of influenza A virus infection within the human respiratory tract. Plos Comp. Biol. 16 (4), e1007705. http://dx.doi.org/10.1371/journal.pcbi.1007705.

Sagi, C., Assaf, M., 2019. Time distribution for persistent viral infection. J. Stat. Mech. 063403. http://dx.doi.org/10.1088/1742-5468/ab1dd7.

Simmonds, P., Aiewsakun, P., Katzourakis, A., 2019. Prisoners of war — host adaptation and its constraints on virus evolution. Nat. Rev. Microbiol. 17 (5), 321–328. http://dx.doi.org/10.1038/s41579-018-0120-2.

Yang, X., Steukers, L., Forier, K., Xiong, R., Braeckmans, K., Reeth, K.V., Nauwynck, H., 2014. A beneficiary role for neuraminidase in influenza virus penetration through the respiratory mucus. Plos One 9 (10), e110026. http://dx.doi.org/10.1371/journal.pone.0110026.

Zitzmann, C., Kaderali, L., 2018. Mathematical analysis of viral replication dynamics and antiviral treatment strategies: From basic models to age-based multi-scale modeling. Front. Microbiol. 9, 1546. http://dx.doi.org/10.3389/fmicb.2018.01546.